Basrah Journal for Engineering Sciences, Vol. 26, No. 1, (2026), 67-78

BJES Basrah Journal for Engineering Sciences

Original Article

Journal homepage: https://bjes.edu.iq/bjes
ISSN (Online): 23118385, ISSN (Print): 18146120

IRAQI Academic Scientific Journals

Investigate the Combined Effect of Various Crude Oil Sulphur Content Levels and Welding Parameters on the Mechanical Properties of API 5L X60 Steels

Muslim Qasem Abdulredah [1]*, Haider Mahdi Lieth [2]

[1] *Department of Material Engineering, College of Engineering, University of Basrah, Basrah, Iraq*
[2] *Department of Mechanical Engineering, College of Engineering, University of Basrah, Basrah, Iraq*
E-mail addresses: muslim.qasemm@uobasrah.edu.iq , haider.lieth@uobasrah.edu.iq

Article Info

Article history:
Received: 8 May 2026
Revised: 10 July 2026
Accepted: 25 July 2026
Published: 28 July 2026

Keywords:
API 5L X60, Sulphur content, Welding parameters, Tensile strength, Hardness, SEM, EDS, XRD.

https://doi.org/10.33971/bjes.26.1.8

Abstract

This study is focused on the assessment of the effects of Sulphur percentage in submerged arc welded API 5L X60 steel under conditions simulated to crude oil environments on its mechanical properties and microstructure. This involved immersing welded specimens in distilled water containing high (0.3250 ml/4L distilled water) and low (0.25 ml/4L distilled water) Sulphur concentrations for four weeks, while unimmersed samples were used as controls for comparison between the two groups of samples. The related experiments were tensile test, hardness measurements, SEM and EDS analyses and XRD analysis. The most mechanically degraded was the high- Sulphur group (H-group); yield strength of 441 MPa (17% loss) and ultimate tensile strength of 506 MPa (11% loss). For the low-sulfur group (L-group), reductions were more moderate: 467 MPa and 523 MPa, respectively. Weld metal (WM) and HAZ hardness values in the H-group were 203 HB and 208 HB, respectively, while those of the L-group were 208 HB and 214 HB. The H-group created a non-protective mixed layer of acicular iron oxides and iron sulfides (FeS) with respect to the microstructural aspects, whereas the L-group developed a thin protective film of iron oxide free from sulfides. Welding parameters were investigated for their effect on the corrosion rate and mechanical properties.

1. Introduction

Although crude oil is still one of the main sources of world energy, pipelines for its transport are highly susceptible to corrosion [1]. Corrosion is often caused by the reaction of Sulphur compounds with iron under higher temperature and the deposition of iron sulfide in pipe inner surface [2]. Crude oil includes Sulphur, Nitrogen, and Oxygen; those with a low Sulphur content are classified as "sweet" crude ($\leq$ 0.5 wt% S), while high-Sulphur oils are grouped as "sour" [3]. Sulphur compounds lead to corrosive hydrogen sulfide (H_2S) production during refining and transport [4], which accelerates iron sulfide scale formation. This leads to reduced integrity of the pipeline, pitting over time which in turn may lead to unstable scales formation [5, 6]. Regarding the abundant reserves of oil in Iraq and the crude oil refineries upgrading, which provide an opportunistic factor for Sulphur-induced corrosion to take a deeper understanding of the Sulphur effects on API 5L X60 steel is based on a systematic strategic importance [7, 8].

1.1. API 5L pipeline steel

API Specification 5L: 2 Standards for steel line pipe. The X grades titles apply to progressively higher classifications of strength, for example PSL 2 defines more rigorous requirements than PSL 1 for demanding operating environments [9, 10]. API 5L X60 is a low-alloy carbon steel widely used in transmission pipelines for its good performance in strength, weldability and cost.

1.2. Application of submerged arc welding (SAW)

Due to its high deposition rates, stable arc characteristics and deep weld penetration, Submerged Arc Welding (SAW) is widely used for pipeline fabrication. In SAW, a wire electrode that is constantly fed (AW) travels under a blanket of granular flux, which protects the molten weld pool from atmospheric contamination [11, 12]. Parameters (e.g. welding current, voltage, travel speed and heat input) which influence the mechanical properties and corrosion resistance of the weld significantly. Finer grain structures in the weld metal and heat-affected zone (HAZ) are achieved with higher welding speeds resulting in lower heat inputs which finally improve mechanical and corrosion performance. On the other hand, excessive heat input coarsens the grains in HAZ and make it more prone to corrosion [13, 14]. This is why SAW parameter optimization is necessary to achieve production of sour-service grades with no defects.

1.3. Current work objectives

In this study, the mechanical properties and hardness of API 5L X60 steel welded in sulfur concentrations that simulate crude oil conditions will be studied. The main objectives are:

© 2026 the Authors. Published by the University of Basrah. Peer-review powered by Elsevier's Editorial Manager ®. This is an open-access article distributed under the Creative Commons Attribution License 4.0.

1. Optimization of welding parameters: A study using three different submerged arc welding (SAW) parameters (voltage, current, and welding speed) and sulfur content to analyze their combined impact on corrosion resistance and mechanical properties.
2. Assessment of tensile properties: To compare between the high-Sulphur (H-group), low-sulfur (L-group) and unimmersed controls in terms of percentage loss of yield strength, ultimate tensile strength and ductility.
3. Macrohardness distribution of weld metal, heat-affected zone (HAZ) and base metal with different coatings was analyzed by comparison between H-group and L-group specimens.
4. Microstructural characterization: SEM, EDS, and XRD to identify corrosion products (iron oxides vs. iron sulfides) and correlate these phases with changes in mechanical properties.

2. Experimental work

2.1. Base metal chemical analysis

The base metal used in this study is API 5L X60 carbon steel, obtained from local oil companies in Basrah Governorate. Both chemical analysis and tensile testing were performed to ensure that the metal used in the study is API 5L X60 Chemical composition analysis was performed according to ASTM A751-14 [15]. using a SPECTROTEST TXC25 spectrum analyzer at the University of Basrah. The results confirmed that the material meets API 5L X60 specifications, with actual composition detailed in Table 1 [16].

Table 1. Chemical composition analysis [15, 16].

X60	C	MN	P	S	Si	Ni	Cr	Cu	V	Ti
	MAX.	MAX.	MAX.	MAX.	MAX.	MAX.	MAX.	MAX.	MAX.	MAX.
Standard [16, 17]	≤ 0.26%	≤ 1.40%	≤ 0.03%	≤ 0.03%	≤ 0.4%	≤ 0.50%	≤ 0.50%	≤ 0.50%	≤ 0.10%	≤ 0.06%
Actual	0.078	1.39	C<0.003	C<0.002	0.251	0.116	0.013	0.014	0.019	0.015

2.2. Crude oil sulphur content analysis

New crudes samples were taken from a number of Iraqi refineries in Basra, Samawa, Maysan Najaf and Nasiriyah In addition to Northern Iraq. X-Ray Fluorescence (XRF) analysis was used to determine Sulphur content. Flash point, density and viscosity were some of the other physical properties recorded. Results indicated significant variations of Sulphur content in which Samawa crude had the highest value (4.7899 wt%) while Basra crude recorded lowest value (3.0261 wt%). Corrosive solutions used in immersion tests thereafter were prepared on the basis of these two samples

2.3. Specimens preparation

Steel plates of measurements 15 cm × 30 cm were used which were cut to smaller specimens as per the test requirements: Immersion test specimens: 5.5 cm × 1 cm × 1 cm (total of 36 specimens), Tensile test samples: manufactured in accordance with the ASTM E8-E8M specification (54 samples), Microstructural specimens: for SEM, EDS and XRD analyses each specimen was ground stepwise with emery papers with 200 to 2000 grit, and polished to leave a lustrous smooth surface in compliance of guidelines from the American Society of Testing Materials (ASTM E3 & ASTM G1-03) [17,18].

2.4. Welding parameters

Controlled parameters of the process were observed during the procedure, including welding speed, current intensity and voltage as shown in Table 2. The samples were selected using a method a full factorial design where the samples are divided into two equal groups. Each sample in the first group has the same parameters as the corresponding sample in the second group. For example, sample 1 has certain parameters, and at the same time, sample 10 has the same parameters. The first is immersed in a high concentration, while the second is immersed in a low concentration, and this applies to the other samples in the table as well.

Table 2. Welding parameters.

No. of samples	Voltage (V)	Current (A)	Speed (mm/s)
1	35	560	21
2	35	590	31
3	35	530	21
4	35	590	21
5	35	530	31
6	35	530	21
7	35	590	31
8	35	530	31
9	35	560	31
10	35	560	21
11	35	590	21
12	35	560	31
13	33	590	21
14	33	560	21
15	33	560	31
16	33	590	21
17	33	530	21
18	33	560	31
19	33	530	31
20	33	530	21
21	33	530	31
22	33	590	31
23	33	560	21
24	33	590	31
25	30	590	31
26	30	560	21
27	30	530	21
28	30	530	31
29	30	530	21
30	30	590	31
31	30	560	31
32	30	560	31
33	30	530	31
34	30	590	21
35	30	590	21
36	30	560	21

Additionally, there is a set of samples with the same welding parameters but not immersed, which were taken as a reference for comparison purposes.

2.5. Welded samples preparation

The study performed at Al-Shuaiba Refinery in Basra, Iraq, by various welding processes represented by Submerged Arc Welding (SAW). The edges of the steel plate were beveled to provide a suitable weld groove. Three-six welding parameter combinations were utilized employing voltage between 30-35 V; current from 530-590 A and weld speed from 21 to 31 mm/s as well as sample with high or low concentrations of Sulphur were welded using the same set of parameters in order ensure homogeneity across specimens.

3. Results and discussion

3.1. Preparation of hostile (corrosive) conditions

Based on the Sulphur content analysis of crude oil (highest 4.7899 wt% and lowest 3.0261 wt%), two sulphuric acid (H_2SO_4) solutions were prepared using the dilution law ($C_1V_1 = C_2V_2$):

- High concentration (H-group): 0.3250 ml H_2SO_4 diluted in 4 liters of distilled water
- Low concentration (L-group): 0.2500 ml H_2SO_4 diluted in 4 liters of distilled water

These solutions simulate the corrosive environment caused by Sulphur compounds in crude oil. Welded specimens were fully immersed for 4 weeks (28 days) at room temperature. Unimmersed welded specimens were kept as reference samples for comparison.

Table 3. Sulphuric acid solution concentrations [4-6].

Sample Location	Sulphur Content (wt%)	Flash Point (°C)	Density (g/cc at 15°C)	Viscosity (cSt at 50°C)
Maysan	4.4582	92	0.9699	196
Najaf	4.1454	90	0.9578	150
Nasiriyah	4.4984	118	0.9647	184
Sayni	3.5096	90	0.9412	72
Dura	4.5043	102	0.9611	184
Bazyan	3.9429	118	0.9602	190
Baiji	3.8357	128	0.9564	163
Samawa	4.7899	129	0.9722	318
Kar	3.8352	102	0.9522	123
Kassak	4.0328	100	0.9654	219
Basra	3.0261	< 20	0.8873	13.4
Gayara	3.0302	126	0.9738	226

3.2. Weight loss

Conduct the weight loss procedure by immersing the first group of samples in a high concentration, as shown in Table 4, and the second group, which has the same welding parameter values, in a low concentration, as illustrated in the Table 5.

3.3. Effect of welding parameters and sulphur media on corrosion and mechanical properties

The results clearly demonstrate the strong interaction between welding parameters and different environments containing varying Sulphur content in determining the corrosion resistance and mechanical performance of API 5L X60 steel. The effect of welding parameters can be attributed primarily to their direct influence on heat input, cooling rate, grain fineness, phase distribution within the weld metal, and the heat-affected zone (HAZ). Increasing the welding speed from 21 mm/s to 31 mm/s resulted in a reduction of heat input per unit length, leading to a finer ferritic microstructure and a narrower HAZ. It is well-established that grain fineness improves mechanical properties and corrosion resistance, as finer grains increase grain boundary density, promoting the formation of more homogeneous and cohesive inert layers while simultaneously reducing localized galvanic variations within the microstructure. Consequently, the samples welded at the higher speed exhibited superior corrosion resistance and retained better mechanical properties after exposure. Higher voltage increases heat input, widens the HAZ, and coarsens grain structure, reducing mechanical properties. Lower voltage produces a finer microstructure and better hardness distribution. Higher current improves penetration but excessive current causes grain coarsening, lowering tensile strength and corrosion resistance. Moderate current with optimized voltage maintains balanced heat input, preserving both mechanical integrity and corrosion performance. Thus, controlling voltage and current is essential to minimize sulfur-induced corrosion and enhance the mechanical behavior of welded API 5L X60 steel.

3.4. Mechanical properties

3.4.1. Tensile test

Tensile tests were conducted on separate samples subjected to the same experimental parameters namely, high and low Sulphur concentrations (S), a four-week immersion time, and the same welding parameters as those investigated via scanning electron microscopy (SEM) analysis combined with energy dispersive spectroscopy (EDS), and X-ray diffraction (XRD) [12, 14]. The results are indicative of a considerable loss in mechanical property due to exposure to the corrosive environment. The yield strength of samples with high Sulphur exposure averaged 441 MPa (ultimate tensile strength 506 MPa) indicating reductions of about 17% and 11%, respectively, when comparing with unimmersed welded references which showed a yield strength and ultimate tensile strength values of sample with yield/ultimate tensile strengths around 534 MPa/569 MPa. Yield strength and ultimate tensile strengths for samples exposed to low Sulphur concentration show an average yield strength of 467 MPa (13% reduction) and an ultimate tensile strength of 523 MPa (8% reduction), respectively, which is comparatively less severe than other treatments as shown in Figs. 1 and 2.

The ability for mixed iron oxide and iron sulfide corrosion products to form was confirmed via SEM and EDS and likely explains the more significant drop in mechanical properties noted in the high Sulphur concentration samples [19]. These products weaken the surface layer, leaving a porous cross section that further promotes corrosion and reduces the net-bearing area.

Table 4. The corrosion rate and weight loss for high Sulphur concentration API 5L (X60).

Sample	Media	NO.	Weights (g)					WΔ (g)	CR (mm/y)
			Original	After immersion					
				1 Week	2 Week	3 Week	4 Week		
X60	Solution one High concentration (HC)	1	42.2843	42.271	42.2461	42.2442	42.233	0.0513	0.118
		2	43.78	43.765	43.753	43.7398	43.7134	0.0666	0.152
		3	43.008	42.9838	42.9741	42.9669	42.9434	0.0646	0.148
		4	41.2903	41.2799	41.2646	41.2554	41.2363	0.054	0.124
		5	43.3768	43.3455	43.3262	43.3189	43.307	0.0698	0.16
		9	43.4788	43.465	43.4504	43.4447	43.4257	0.0531	0.122
		13	41.7607	41.7478	41.735	41.725	41.7008	0.0599	0.137
		14	42.5694	42.5534	42.5423	42.5307	42.5137	0.0557	0.128
		15	42.6787	42.6693	42.6605	42.6521	42.6288	0.0499	0.114
		17	42.6383	42.6235	42.6129	42.5942	42.5795	0.0588	0.135
		19	43.5969	43.5738	43.5613	43.5353	43.5275	0.0694	0.159
		22	43.0083	42.993	42.9903	42.972	42.9503	0.058	0.133
		25	46.5383	46.5031	46.482	46.453	46.4337	0.1046	0.239
		26	46.2995	46.2778	46.253	46.2377	46.2281	0.0714	0.164
		27	44.9369	44.9148	44.8931	44.8814	44.8735	0.0634	0.145
		28	42.3421	42.3159	42.2927	42.2807	42.2707	0.0714	0.164
		31	45.318	45.2878	45.263	45.2463	45.2407	0.0773	0.177
		34	45.7721	45.7449	45.7238	45.7113	45.711	0.0611	0.14

Table 5. The corrosion rate and weight loss for low Sulphur concentration API 5L (X60).

Sample	Media	NO.	Weights (g)					WΔ (g)	CR (mm/y)
			Original	After immersion					
				1 Week	2 Week	3 Week	4 Week		
X60	Solution two Low concentration (LC)	10	43.2135	43.2031	43.181	43.1739	43.143	0.0705	0.0212
		7	43.1213	43.1061	43.0835	43.9746	43.0541	0.0672	0.0202
		6	43.3351	43.3205	43.3014	43.2902	43.2643	0.0708	0.0213
		11	43.1788	43.1634	43.137	43.1343	43.1128	0.066	0.0198
		8	40.9658	40.9432	40.929	40.9209	40.9022	0.0636	0.0191
		12	41.5318	41.5181	41.4982	41.4892	41.467	0.0648	0.0195
		16	41.971	41.9445	41.9288	41.9221	41.9047	0.0663	0.0199
		23	42.2608	42.2463	42.2259	42.2207	42.1957	0.0651	0.0196
		18	42.4257	42.4056	42.3872	42.375	42.3596	0.0661	0.0199
		20	43.5364	43.5228	43.505	43.4999	43.4766	0.0598	0.018
		21	42.6893	42.6724	42.6527	42.6445	42.622	0.0673	0.0202
		24	44.6085	44.5998	44.5749	44.5648	44.5454	0.0631	0.019
		30	40.1586	40.1484	40.1279	40.118	40.0977	0.0609	0.0183
		36	46.2315	46.2094	46.187	46.1773	46.1582	0.0733	0.022
		29	45.8455	45.8258	45.8007	45.7945	45.776	0.0695	0.0209
		33	43.535	43.5271	43.4849	43.481	43.461	0.074	0.0223
		32	41.4958	41.4951	41.4772	41.4675	41.456	0.0398	0.012
		35	42.9233	42.9038	42.8879	42.8772	42.8571	0.0662	0.0199

In contrast, the low Sulphur concentration samples created only thin, relatively protective films of iron oxide with no greater quantities of sulfides detectable on the surface, reducing mechanical degradation. This means that the tensile and microscopic samples were not exactly the same, but due to them being prepared and exposed under identical surface conditions, a reasonable correlation between corrosion morphology and mechanical behavior could be made. These outcomes highlight that the formation of sulfidation products (FeS/FeS_2) can expedite degradation in mechanical properties far more than oxidation alone.

Table 6. Tension test of API 5L X60 for H & L concentration samples.

Sample No.	Immersed Samples				Not Immersed	
	Yield		Ultimate		Yield	Ultimate
	High concentration	How concentration	High concentration	How concentration		
1 & 10	374	381	451	462	574	604
2 & 7	445	469	528	551	510	523
3 & 6	398	407	477	482	553	622
4 & 11	385	428	473	512	508	594
5 & 8	398	413	477	488	492	495
9 & 12	420	442	490	519	556	618
13 & 16	406	437	470	515	517	595
14 & 23	407	500	486	556	533	550
15 & 18	402	460	480	549	525	555
17 & 20	388	462	444	544	535	609
19 & 21	391	432	454	510	541	573
22 & 24	418	556	478	583	588	597
25 & 30	551	441	559	445	513	580
26 & 36	535	486	606	555	548	588
27 & 29	502	435	561	438	577	618
28 & 33	523	544	567	613	419	419
31 & 32	521	525	606	575	540	541
34 & 35	490	533	501	588	521	523

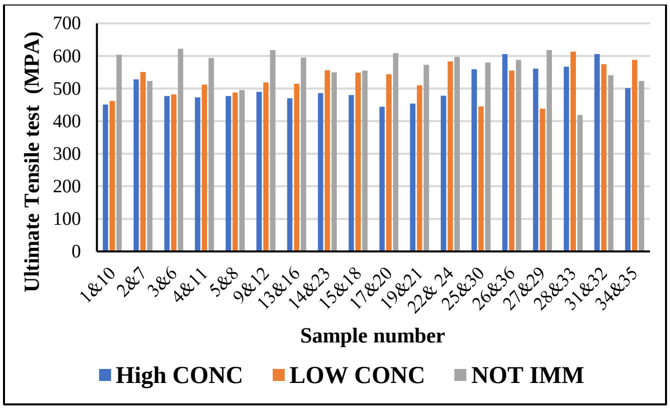

Fig. 1 Ultimate tensile test for X60 in H, L & not immersed concentration.

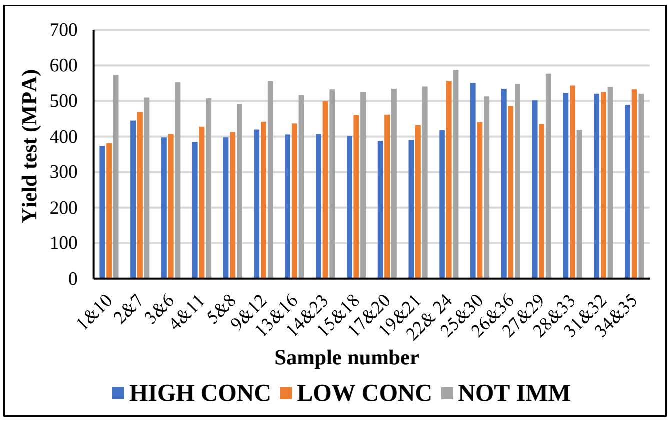

Fig. 2 Yield test for X60 in H, L & not immersed concentration.

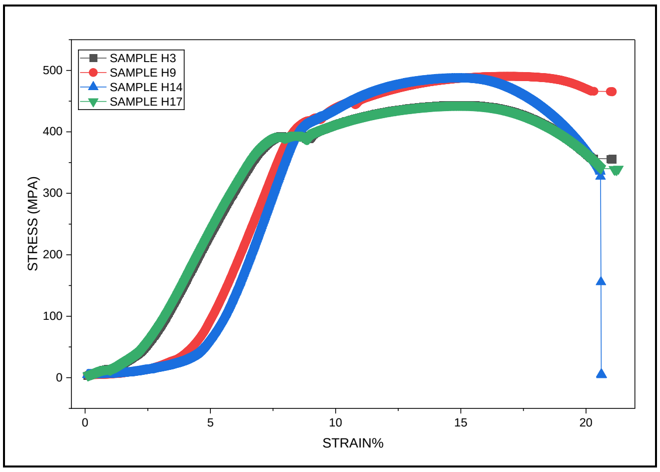

Fig. 3 Tensile test for X60 in high concentration.

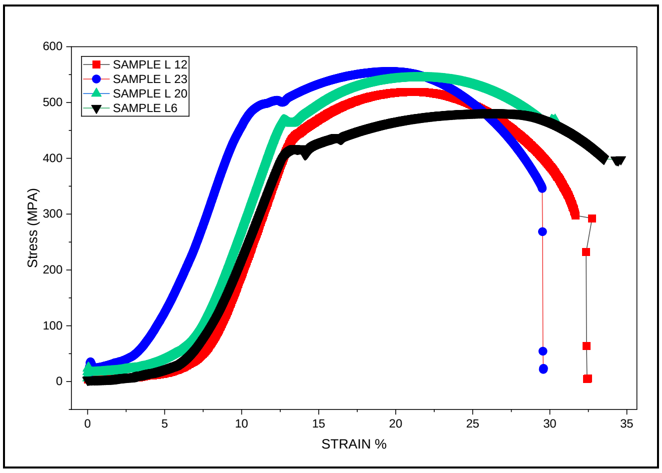

Fig. 4 Tensile test for X60 in low concentration.

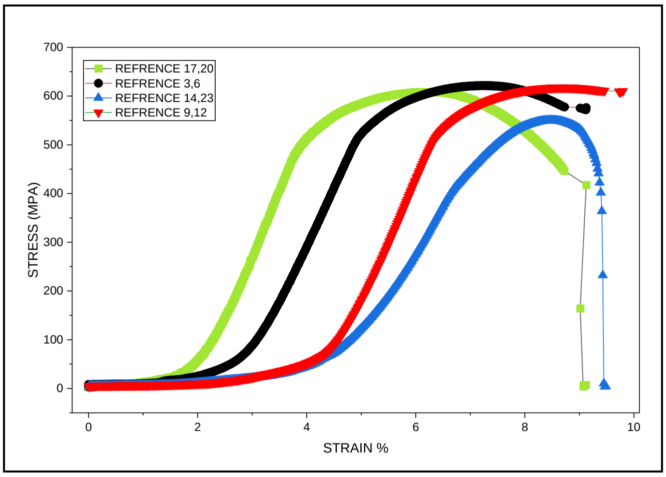

Fig. 5 Tensile test for reference sample.

3.4.2. Hardness test

1. H-Group (High Sulphur Concentration)

- *Average hardness values*

1. Weld metal: 203 HB.
2. Heat-affected zone (HAZ): 208 HB.

The weld metal and HAZ hardness are greater than the base metal in the H-group (high Sulphur concentration), due to thermal cycling and microstructural refinement that occurs as a result of welding. However, these regions in the H-group are slightly less hard than equivalent regions from the L-group. The decrease is mainly due to non-protective iron sulfide (FeS) phases resulting from the excessive Sulphur concentration [13]. These sulfides are weak points in the microstructure and weaken the hardness as a whole. The variability in hardness seen for the individual H-group samples weld metal hardness from 237 HB in sample 17 to 170 HB was found in sample 2 can be attributed to differences in welding parameters (e.g., voltage, current and travel speed) that affect grain size and thermal history (see Fig. 6).

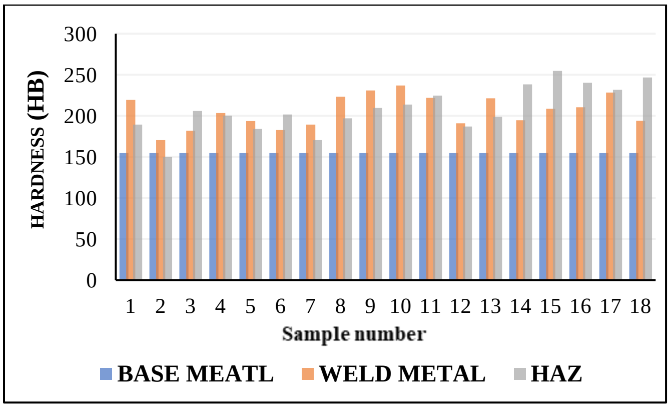

Fig. 6 Hardness test for H-Group.

2. L-Group (Low Sulphur Concentration)

- *Average hardness values*

1. Weld metal: 208 HB.
2. Heat affected zone (HAZ): 214 HB.

L Group shows low Sulphur which results in both the weld metal and HAZ having higher hardness values than the H-Group. The low Sulphur environment encourages only very mild oxidation in which only a thin iron oxide film is formed as opposed to those undesirable iron sulfides. The absence of sulfide-related degradation allowed the hardening mechanisms arising from welding such as grain refinement and phases transformation to remain active. The slightly harder HAZ compared to the weld metal is a normal metallurgical response, consisting of fine-grained and tempered microstructures. The variability for the L-group (i.e., sample 35 with 255 HB in the HAZ; versus sample 16 with 169 HB in the HAZ) is attributable to changes in welding process parameters [13, 14].

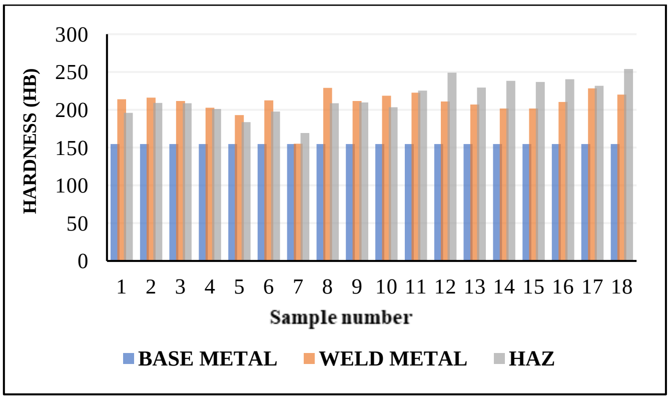

Fig. 7 Hardness test for L-group.

3. *Base metal (unwelded reference)*

For both groups (H-group and L-group), the average hardness of base metal (BM) in samples of API 5L X60 steel did not modify significantly and was equal to 155 HB. This uniform hardness not only assures the homogeneity of the as-received material, but also provides a reliable unwelded comparison [16].

3.5. Microstructure analysis

Scanning Electron Microscope (SEM) is a high magnification tool for surface morphology and microstructure studies. The topography is revealed in clear detail, including grains, boundaries, cracks, pits and porosity. To be effective at imaging, SEM requires samples to be conductive or have a coating of gold/carbon on non-conductive materials. In addition to SEM, Energy Dispersive X-ray Spectroscopy (EDS) is an analytical technique that identifies elemental composition qualitatively and semi-quantitatively. This is achieved by means of point analysis, line scanning, and elemental mapping that may see corrosion products and alloying elements but lacks sensitivity to lighter elements. X-ray Diffraction (XRD) is furthermore a non-destructive method used to give information about crystalline phases in a certain sample.

Table 5. Distribution of tested samples for SEM, EDS, and XRD analyses.

Test	Sample	Immersed		Non-Immersed
		No. of Samples	No. of Samples	
SEM	AS CAST	1, 9	10, 12	10, 12
EDS	AS CAST	1, 9	10, 12	10, 12
XRD	AS CAST	1, 9	10, 12	10, 12

It can identify specific compounds, like iron carbonate ($FeCO_3$) from CO_2 corrosion or iron sulfide (FeS) from H_2S corrosion [18]. This tool also allows us for the semi-quantitative phases analysis and gives information about the crystallite size.

As previously mentioned, three samples immersed in high concentration and three others in low concentration were examined, in addition to the analysis of non-immersed samples for comparative purposes, as well as the metal as cast. Furthermore, the corrosion residues collected from the high and low concentration solutions were also analyzed. EDS, SEM, and XRD examinations were conducted.

Table 7. Hardness test for H-group (high Sulphur concentration).

Sample No.	Base metal			Average	Weld metal			Average	HAZ			Average
1	163	151	150	154.6667	217	220	221	219.3333	215	175	178	189.3333
2	163	151	150	154.6667	176	170	165	170.3333	151	149	150	150
3	163	151	150	154.6667	159	197	190	182	217	191	210	206
4	163	151	150	154.6667	211	198	201	203.3333	204	199	198	200.3333
5	163	151	150	154.6667	211	180	190	193.6667	174	190	188	184
9	163	151	150	154.6667	186	180	182	182.6667	197	205	203	201.6667
13	163	151	150	154.6667	165	245	158	189.3333	188	151	172	170.3333
14	163	151	150	154.6667	220	224	226	223.3333	200	198	193	197
15	163	151	150	154.6667	226	236	231	231	210	209	210	209.6667
17	163	151	150	154.6667	233	230	248	237	215	210	216	213.6667
19	163	151	150	154.6667	217	227	222	222	218	237	219	224.6667
22	163	151	150	154.6667	191	190	192	191	182	191	188	187
25	163	151	150	154.6667	224	221	219	221.3333	210	190	197	199
26	163	151	150	154.6667	206	188	190	194.6667	216	259	240	238.3333
27	163	151	150	154.6667	214	204	208	208.6667	265	248	251	254.6667
28	163	151	150	154.6667	215	207	209	210.3333	242	240	239	240.3333
31	163	151	150	154.6667	208	256	221	228.3333	220	242	233	231.6667
34	163	151	150	154.6667	189	200	193	194	243	252	245	246.6667

Table 8. Hardness test for l-group (low Sulphur concentration).

Sample No.	Base metal			Average	Weld metal			Average	HAZ			Average
10	163	151	150	154.6667	217	215	210	214	193	198	197	196
7	163	151	150	154.6667	219	220	209	216	201	215	211	209
6	163	151	150	154.6667	217	207	211	211.6667	200	215	211	208.6667
11	163	151	150	154.6667	211	195	202	202.6667	204	200	199	201
8	163	151	150	154.6667	210	179	190	193	174	190	187	183.6667
12	163	151	150	154.6667	210	213	214	212.3333	204	206	183	197.6667
16	163	151	150	154.6667	166	143	156	155	188	150	170	169.3333
23	163	151	150	154.6667	234	225	228	229	204	214	208	208.6667
18	163	151	150	154.6667	215	208	212	211.6667	212	209	208	209.6667
20	163	151	150	154.6667	198	228	230	218.6667	199	200	211	203.3333
21	163	151	150	154.6667	217	228	223	222.6667	218	238	220	225.3333
24	163	151	150	154.6667	200	218	215	211	236	261	250	249
30	163	151	150	154.6667	205	214	202	207	252	219	217	229.3333
36	163	151	150	154.6667	198	207	200	201.6667	207	249	259	238.3333
29	163	151	150	154.6667	206	198	201	201.6667	249	228	233	236.6667
33	163	151	150	154.6667	215	207	209	210.3333	242	240	239	240.3333
32	163	151	150	154.6667	208	256	221	228.3333	220	242	233	231.6667
35	163	151	150	154.6667	222	218	220	220	248	259	255	254

The scanning electron microscope (SEM) micrographs are observed at different magnificences from X300 to X10000, which confirm the topography of a base metal detected in API 5L X60 forms with no welding or corrosion exposure. At the lower magnifications (X300 to X600), the surface appears smooth and homogeneous, disclosing fine parallel grinding or rolling marks representative of the as-manufactured condition, and presents no indication of corrosion products, pitting or irregular deposits. At intermediate magnifications (X1300, X2500), the surface retains a more homogeneous appearance and consists only of minor fine particulates from sample preparation and shows no signs of oxidation nor contamination that are beyond a native air-formed oxide film shown in Fig. 8. No acicular structures, porous layers, sulfide phases or corrosion-related features are observed at higher power (X5000 to X10000) which further confirms the absence of corrosion attack. This is confirmed from energy dispersive spectroscopy (EDS) analyses where iron is determined as the main element however the traces elements are normally associated with API 5L X60 steel. Notably, Sulphur is not detected, further corroborating the absence of sulfides. Each XRD pattern consists of narrow and intense peaks that are typical for body-centered cubic (BCC) ferritic iron in a low-carbon steel, with no observable significant peaks from oxides or sulfides confirming that the surface is clean and unreacted. This base metal sample is important to reference for the effects of welding only (not immersed welded samples) and the combined effects of welding and exposure to H_2SO_4 (immersed samples) shown Fig. 10. The differences in microstructure or composition identified in the welded or exposed specimens can now clearly be assigned to either the weld process or to exposure in this corrosive medium.

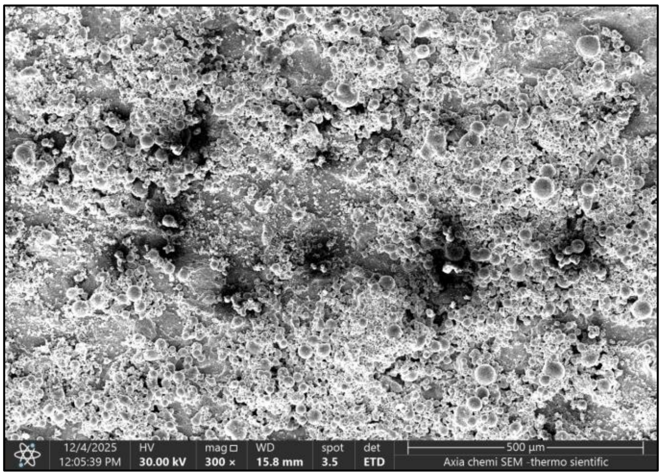

Fig. 8 Sample AS CAST (500 µm) SEM.

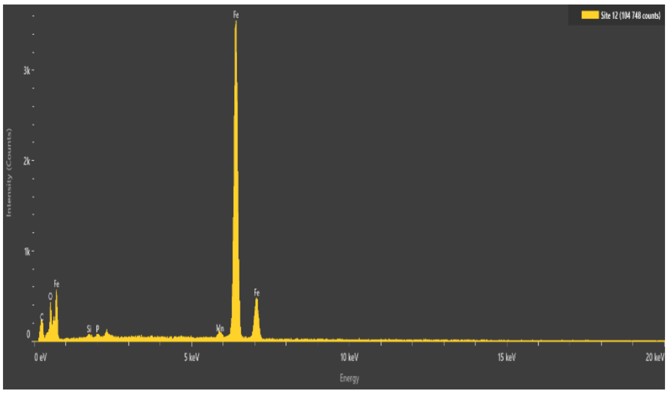

Fig. 9 EDS test to basic metal sample.

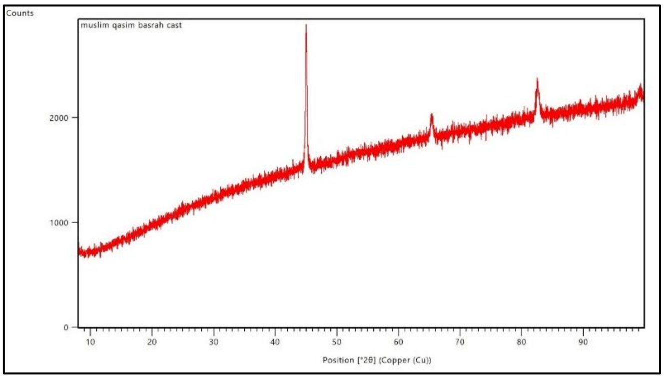

Fig. 10 XRD test to basic metal sample.

3.6. SEM, EDS and XRD test

H1 (High Absorption): SEM micrographs show a rough and irregular surface which is fully covered by corrosion products. High-magnification image (X10000) of an individual blade fiber shows acicular (needle-like) structures consistent with a mixed iron oxide and iron sulfide formation, as shown in Fig. 11.

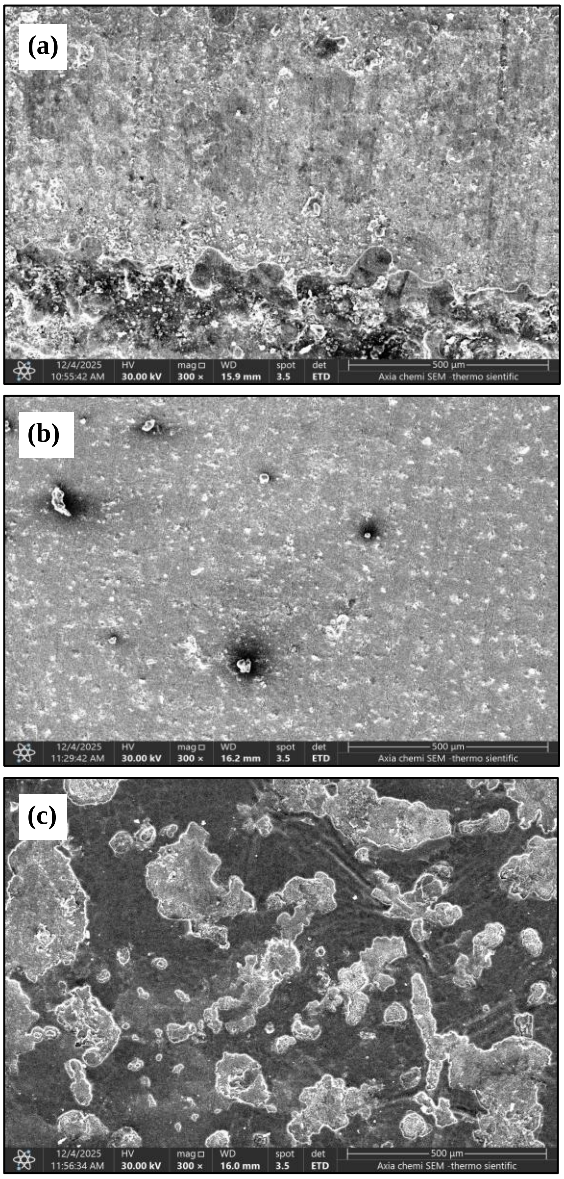

Fig. 11 SEM for **(a)** high concentration **(b)** low concentration **(c)** non immersed.

EDS analysis for S at 2.5 keV along with O and Fe (with corresponding peaks) provides confirmation of the presence of Sulphur, supporting formation of FeS in addition to Fe_2O_3 and Fe_3O_4, as shown in Fig. 12. XRD patterns show resolute iron peaks, distinct oxide peaks and small sulfide peaks further confirming the formation of a mixed, non-protective corrosion layer, as shown in Fig. 13. SEM images from precipitated samples L10 (low concentration) typically, the surface appears relatively smooth or rough and with only a few small corrosion nodules. There are no acicular structures or extensive pitting. EDS shows no Sulphur therefore, it is not subject to sulfidation. Only trace amounts of oxygen are found (indicating the presence of a thin, passivating iron oxide layer). XRD shows metallic iron being the dominant oxygenated phases, and oxide peaks quite weakly as well so no evident sulfide peaks. Sample Ref10: SEM image of the unimmersed reference showing a clean welded surface free from any corrosion products but with slight thermal oxidation due to the welding process. EDS shows no Sulphur and only a trace amount of oxygen. XRD shows only sharp peaks for metallic iron, indicating no substantial corrosion. Sulphur causes presence in H1 gives a coarse, non-protective oxide sulfide layer leading to rapid corrosion. On the other hand, the lack of Sulphur in L10 and Ref10 leads either to a thin, passivating oxide layer (L10) or even absence of corrosion layer (Ref10), providing superior maintenance of surface integrity and mechanical properties.

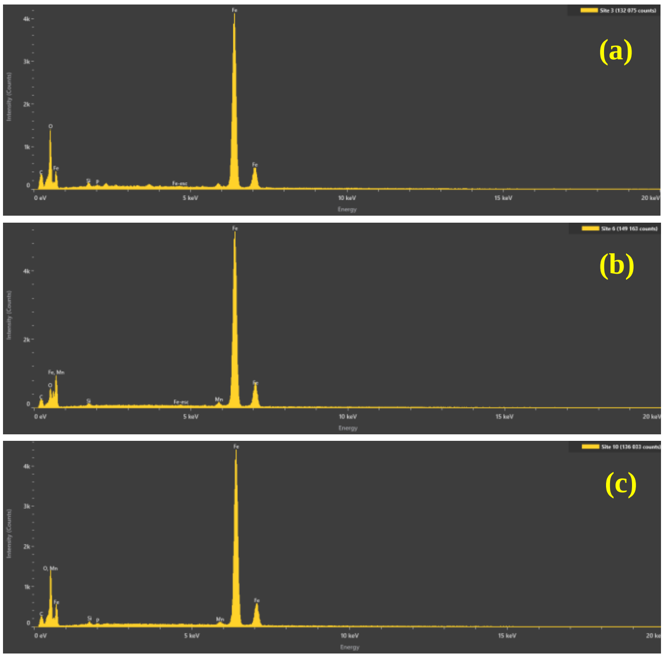

Fig. 12 EDS for **(a)** high concentration **(b)** low concentration **(c)** non immersed.

Sample H9 (High Concentration), the SEM micrographs show a rough surface covered by irregularly distributed corrosion products, but the degree of attack is much lower than Sample H1 under corresponding conditions due to higher welding speed (31 mm/s instead of 21 mm/s). No acicular structures are detected. Although S is detected at 2.5 keV in EDS analysis, there is less intensity than at H1 showing lower sulfidation [5, 6]. The XRD patterns also show well defined iron peaks and distinct oxide peaks with weak or absent sulfide peaks, indicating that oxides are dominant over sulfides.

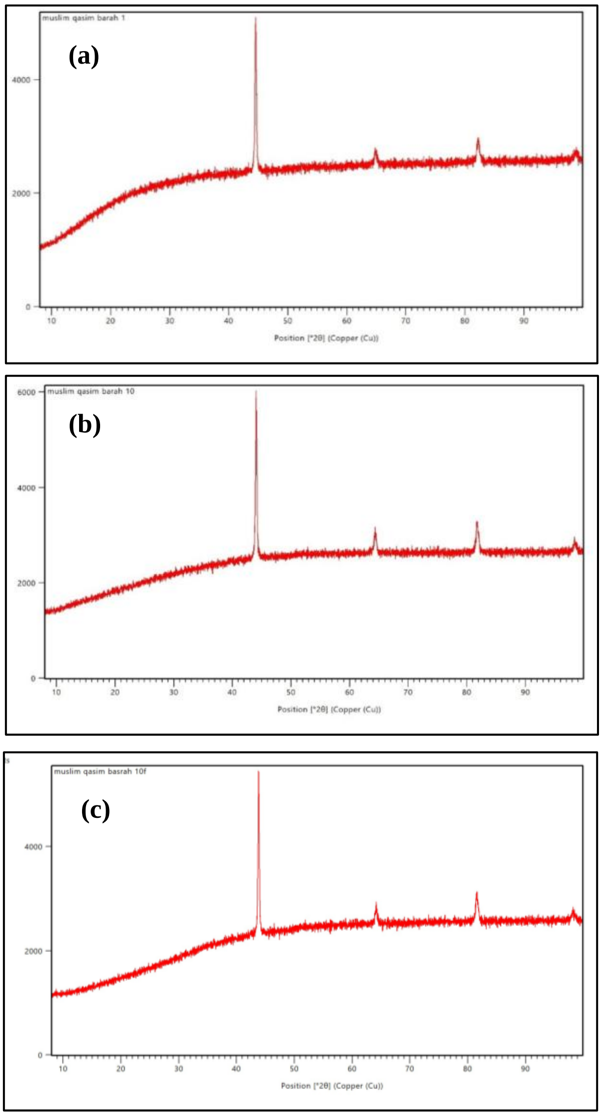

Fig. 13 XRD for **(a)** high concentration **(b)** low concentration **(c)** non immersed.

This increase in welding speed leads to a reduction in heat input, which refines the grain structure of both the weld metal and HAZ, improving corrosion resistance compared with H1. L12 (Low Concentration) Sample SEM images showing in Fig. 14 a reasonably smooth surface with sparse, small corrosion nodules without extensive pitting with the metallic shine of the surface hardly affected. No Sulphur is detected by EDS, indicating a lack of sulfidation only trace oxygen is noted as well in Fig. 15, suggesting that the specimen developed a very thin iron oxide protective layer. The dominant phases appear to be metallic iron, corroborated by a minimal presence of oxide peaks (very weak) and no detectable sulfide peaks using XRD standard analysis (see Fig. 16). Sample Ref12 (Sample are not immersed in solution): SEM observation of the welded surface showed no corrosion products, but minor thermal oxidation from the welding process. Almost no oxygen and no Sulphur found by EDS. XRD spectra show only sharp metallic iron peaks proving absence of significant corrosion. Seeing as Sample H9 was welded at a much faster welding speed (31 mm/s) than H1 and therefore exhibits a finer microstructure, it is not surprising that the corrosion resistance of sample H9 is higher.

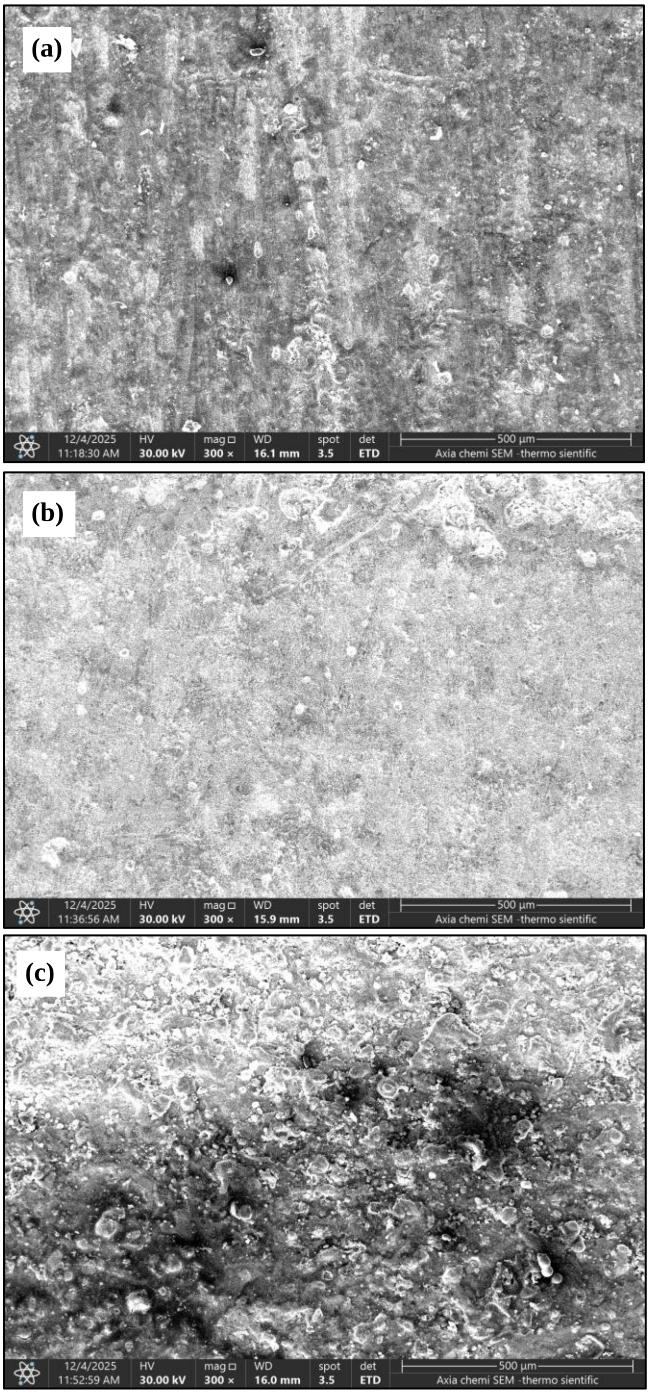

Fig. 14 SEM for **(a)** high concentration **(b)** low concentration **(c)** non immersed.

However, the sulfide species remains, giving rise to a mixed oxide-sulfide layer and this time less represented than in H1. In comparison, Sample L12 is just gently oxidized with no signs of sulfidation while Ref12 shows no corrosion at all. The effects of increasing welding speed as leading to lower heat input have been shown by these findings which increase the corrosion resistance of welded API 5L X60 steel in both high and low concentration H_2SO_4 environment [19].

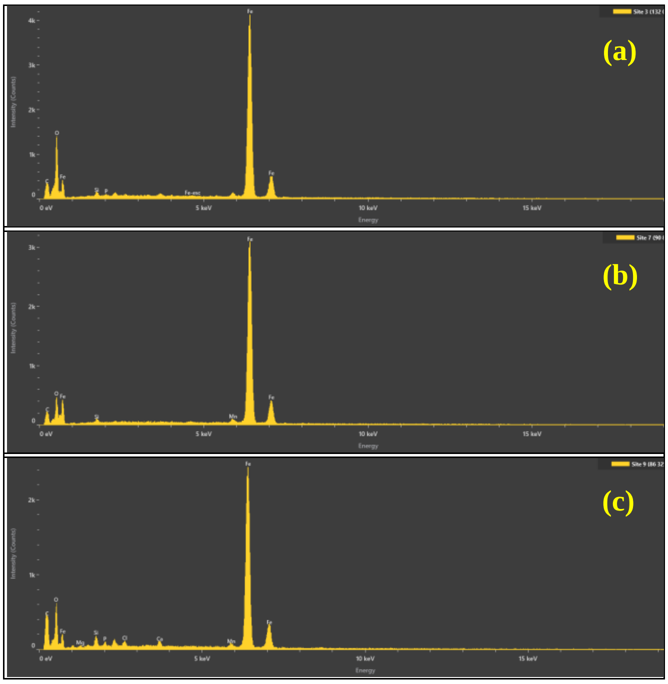

Fig. 15 EDS for **(a)** high concentration **(b)** low concentration **(c)** non immersed.

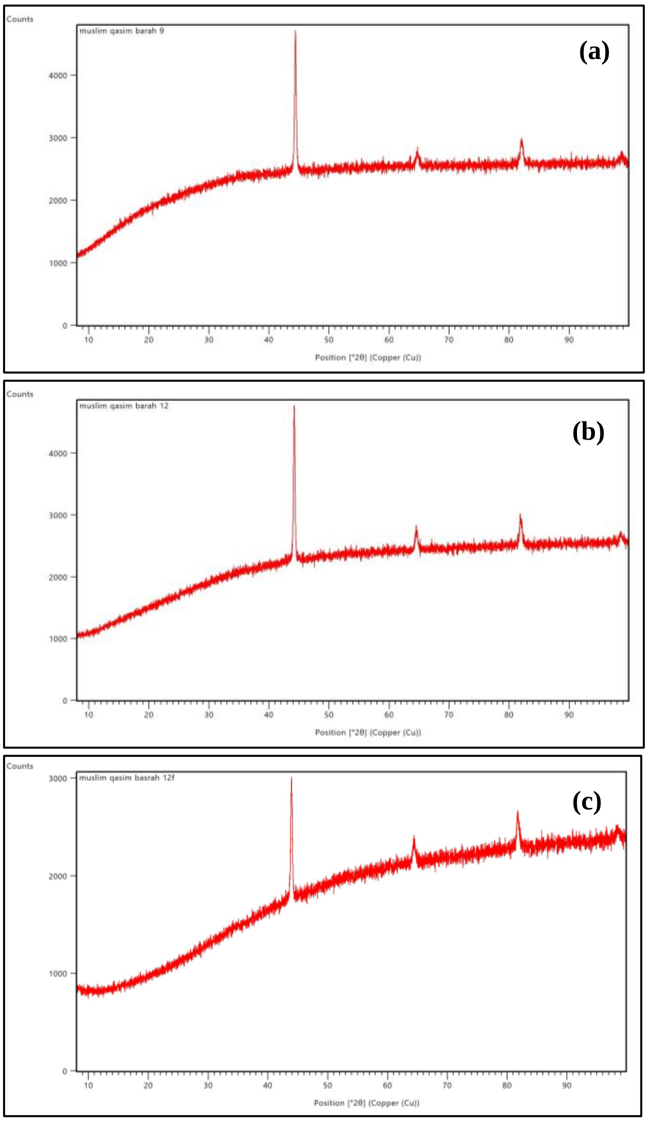

Fig. 16 XRD for **(a)** high concentration **(b)** low concentration **(c)** non immersed.

3.7. XRD Structural comparison between samples and base metal

The only sharp, intense peaks observed in the as-cast base metal XRD pattern (Fig. 10) correspond to those from a body centered cubic (BCC) α-ferrite structure with no indication that any oxides or sulfides were present, indicating a clean, uncorroded surface. Whereas the high-sulfur sample H1 (welded at a speed of 21 mm/s, Fig. 13(a) shows new weak peaks near 30.1° and 50.2° due to iron sulfide (FeS), in addition to oxide peaks at angles of 35.4° and 62.8°, which correspond to magnetite (Fe_3O_4). That indicates a mixed corrosion layer that is not protecting. But at higher welding speed of 31 mm/s in the sample H9, Fig. 16(a), sulfide peaks become very weak or almost are absent, while oxide peaks are preserved that confirms more effective sulfidation reduction at higher welding speed due to lower heat input and grain refinement. Alternatively, for the low sulfur sample L10, Fig. 13(b), only weak oxide signals and no detectable sulfides were observed in a similar manner to that previously discussed, confirming an ultrathin protective iron oxide film formation devoid of FeS phases. Likewise, sample L12, low Sulphur, 31 mm/s, Fig. 16(b), demonstrates a clean trend with a predominance of α-Fe and slightly higher oxide peaks than samples H12 - H20 thus also indicating good corrosion resistance. The XRD patterns of the none-immersed reference samples, Ref10 and Ref12 (Fig. 13(c) and Fig. 16(c)), reveals XRD patterns visually identical to those obtained with the base metal with only sharp α-Fe peaks evident without signs of oxides nor sulfides affirming that practically no corrosion occurred when the specimens were not immersed in sulfurous medium. All the welded samples exhibited slight broadening of their peaks compared to base metal, which can be associated with the residual stresses possibly resulted from the thermal cycles produced during welding as well as cold working due to grain refinement. Furthermore, the principal α-Fe peak is observed at around $2\theta \approx 45°$ in the welded samples, and this has been shifted from its normal position of ~44.5° (standard) due to lattice distortion and residual stress. The main structural difference among all tests is the presence of FeS alone in high-sulfur, slow compositions, which directly correlates to the significant mechanical degradation we see. On the other hand, their higher retention in tensile strength and hardness from both low-sulfur and higher-speed samples is due to that no sulfides were formed. In general, the XRD results provide clear evidence that the base metal has a clean BCC ferritic structure, while the corrosion products range from mixed oxide-sulfide layers in the most aggressive conditions to protective oxide films or complete absence of corrosion layers for low sulfur concentrations, adjusting welding parameters.

4. Conclusion

Based on the experimental results obtained from the investigation of welded API 5L X60 steel immersed in high and low Sulphur concentrations for four weeks, the following conclusions can be drawn:

1. Influence of welding parameters on microstructure: grain size, phase distribution and HAZ width are governed by voltage, current and speed. Grain coarsening and wider HAZ were caused by the use of high voltage and current, while fine, homogeneous microstructures occurred at low parameters.
2. Influence of microstructure on corrosion susceptibility: high surface energy and active grain boundaries of coarse grains wider heat affected zones (HAZs) make turbines more susceptible to corrosion because sulfur combine rapidly with these metals.
3. Dependence of the formation of corrosion products on sulfur concentration: at higher sulfur concentrations, a porous and non-protective layer of iron sulfide (FeS) forms, leading to eventual corrosion. At low concentration they will form a thin oxide layer of (Fe_2O_3/Fe_3O_4) that slows down oxidation.
4. Corrosion impact on mechanical properties: when the corrosion is severe, it considerably reduces the effective cross-section and increase stress concentration at this pitting sites. The same goes with yield strength and ultimate tensile strength which has significantly lower values.
5. Sulfur effect is not absolute: the effect of sulfur is greatly reliant on welding conditions. Voltage and current can actually have a stronger effect on mechanical properties and corrosion rates than concentration of sulfur in some cases.
6. Non-linearity of welding speed effect: weld speed is not always an indication of quality. Where maximum speed cannot produce a likewise optimum result, the materialization process was rather carried out at moderate numerical settings (33 V, 560 A, 21 mm/s).
7. Hardness is not actually an independent indicator of corrosion resistance: corrosion resistance is not solely determined by hardness. Material behavior is much more sensitive to phase distribution and surface layer coherence than one could expect.
8. Microscopy analysis proves that no uniformity in the type of FeS formed: microscopic imaging showed that high sulfur composite forms porous FeS and low sulfur form protective oxides. Welding parameters further influence the corrosion products, since minimum voltage and current can inhibit FeS formation.
9. Statistical analysis must prevail because of misleading average values: averages mask result variability. Future studies could apply statistical tools (standard deviation, ANOVA) to evaluate differences between groups more objectively.
10. This paper demonstrates that Sulphur could harmfully weaken API 5L X60 steel by lowering the impact toughness of HAZ, but this effect can be restrained by adjusting welding parameters to moderate voltage and current so it enables API 5L X60 steel to be made use in sour atmosphere without using costly another alloy instead.

5. Recommendations

Based on the findings of this study, the following recommendations are proposed for industrial practice and future research:

To improve mechanical properties and corrosion resistance in sour service environments, it is recommended to use higher welding speeds (≥31 mm/s) and lower heat input to refine grain structure in the weld metal and heat affected zone (HAZ). For pipelines transporting high Sulphur crude oil, internal coatings or corrosion inhibitors should be considered to mitigate sulfide induced degradation of tensile strength and hardness. Regular mechanical property monitoring (tensile and hardness testing) alongside microstructural analysis

(SEM/EDS/XRD) is advised for early detection of Sulphur induced damage. Future research should focus on longer immersion periods, the combined effect of H_2S and CO_2, elevated temperatures, and post weld heat treatment to further enhance the mechanical performance of welded API 5L X60 steel in aggressive environments.

References

[1] S. Chougle and S. M. Walke, "Generations of Crude Oil," American International Journal of Research in Science, Technology, Engineering & Mathematics, vol. 10, no. 4, pp. 309-313, 2015.

[2] M. Meriem-Benziane, B. Bou-Saïd, and N. Boudouani, "The effect of crude oil in the pipeline corrosion by the naphthenic acid and the sulfur: A numerical approach," Journal of Petroleum Science and Engineering, vol. 158, pp. 672-679, 2017. https://doi.org/10.1016/j.petrol.2017.08.073

[3] G. Yasin, M. I. Bhanger, T. M. Ansari, S. M. S. R. Naqvi, M. Ashraf, K. Ahmad and F. N. Talpur, "Quality and Chemistry of Crude Oils," Journal of Petroleum Technology and Alternative Fuels, vol. 4, no. 3, pp. 53-63, 2013. https://doi.org/10.5897/JPTAF12.025

[4] J. Zhang, Z. Feng, W. Fang, Q. Huo, K. Zhang, J.-K. Li, H.-S. Zeng and B.-W. Zhang, "Crude-oil hydrocarbon composition characteristics and oil viscosity prediction in the northern Songliao Basin," Science China Earth Sciences, vol. 57, pp. 297-312, 2014. https://doi.org/10.1007/s11430-013-4656-8

[5] A. Vetere, D. Pröfrock, W. Schrader, "Qualitative and Quantitative Evaluation of Sulfur-Containing Compound Types in Heavy Crude Oil and Its Fractions," Energy & Fuels, vol. 35, Issue 10, pp. 8723-8732, 2021. https://doi.org/10.1021/acs.energyfuels.1c00491

[6] M. A. Gab-Allah, E. S. Goda, A. B. Shehata, and H. Gamal, "Critical Review on the Analytical Methods for the Determination of Sulfur and Trace Elements in Crude Oil," Critical Reviews in Analytical Chemistry, vol. 50, Issue 2, pp. 161-178, 2020. https://doi.org/10.1080/10408347.2019.1599278

[7] T. AL-Saadi, A. Cherepovitsyn, and T. Semenova, "Iraq Oil Industry Infrastructure Development in the Conditions of the Global Economy Turbulence," Energies, vol. 15, Issue 17, P. 6239, 2022. https://doi.org/10.3390/en15176239

[8] A. Alzahawy, and H. Issa, "The Iraqi Petroleum Refining Industry: A Review of Environmental Impact Assessment. Preprints, 2024. https://doi.org/10.20944/preprints202405.0901.v1

[9] M. L. Nayyar, Piping Handbook, 7th ed. New York, NY, USA: McGraw-Hill, 2000. ISBN 0-07-047106-1

[10] American Petroleum Institute, API Specification 5L: Specification for Line Pipe, 45th ed. Washington, DC, USA: American Petroleum Institute, 2013.

[11] S. Rie, K. Kazuyuki, I. Tooru, N. Yoshihito, and M. Yutaka, "Development of Vertical Submerged Arc Welding Method for Aboveground LNG Storage Tank Construction," IHI Engineering Review, vol. 43, no. 2, pp. 55-62, 2010.

[12] A. Singh and R. P. Singh, "A Review of Effect of Welding Parameters on the Mechanical Properties of Weld in Submerged Arc Welding Process," Materials Today: Proceedings, vol. 26, no. 2, pp. 1714-1717, 2020. https://doi.org/10.1016/j.matpr.2020.02.361

[13] R. P. Singh, A. Singh, and A. Singh, "Optimization of Hardness of Weld in Submerged Arc Welding," Materials Today: Proceedings, vol. 26, no. 2, pp. 1827-1830, 2020. https://doi.org/10.1016/j.matpr.2020.02.382

[14] H. Sharma, B. Rajput, and R. P. Singh, "A Review Paper on Effect of Input Welding Process Parameters on Structure and Properties of Weld in Submerged Arc Welding Process," Materials Today: Proceedings, vol. 26, no. 2, pp. 1931-1935, 2020. https://doi.org/10.1016/j.matpr.2020.02.422

[15] ASTM International, ASTM A751-14, "Standard Test Methods, Practices and Terminology for Chemical Analysis of Steel Products," West Conshohocken, PA, USA, 2014.

[16] I. S. Bott, F. Siciliano, G. Z. Batista, J. M. Gray, "Line Pipe Steels," In: ABCM – Brazilian Society of Mechanical Sciences and Engineering, J. L. de França Freire, M. R. Rennó Gomes, M. Guedes Gomes, (eds) Handbook of Pipeline Engineering, Springer, Cham, 2024. https://doi.org/10.1007/978-3-031-33328-6_9

[17] ASTM International, ASTM E3, "Standard Guide for Preparation of Metallographic Specimens," West Conshohocken, PA, USA, 2011.

[18] ASTM International, ASTM G1-03, "Standard Practice for Preparing, Cleaning, and Evaluating Corrosion Test Specimens," West Conshohocken, PA, USA.

[19] ASTM International, ASTM G5-87, "Standard Reference Test Method for Making Potentiostatic and Potentiodynamic Anodic Polarization Measurements," West Conshohocken, PA, USA.